The 7th International Conference on Chirality, Vorticity and Magnetic Field in Heavy Ion Collisions

Interplay between nuclear structure and the chiral magnetic effect in isobaric collisions

PRC 106, 034909 (2022)

Xin-Li Zhao, Guo-Liang Ma

2023/07/18

Jul 15/19 2023

International Conference Center
University of Chinese Academy of Sciences

Outline

1) Motivation
2) Results and Discussions
   - ✓ N_{ch} & v_2
   - ✓ $\Delta\delta$ & $\Delta\gamma$
3) Summary

Strong Magnetic Field in HIC

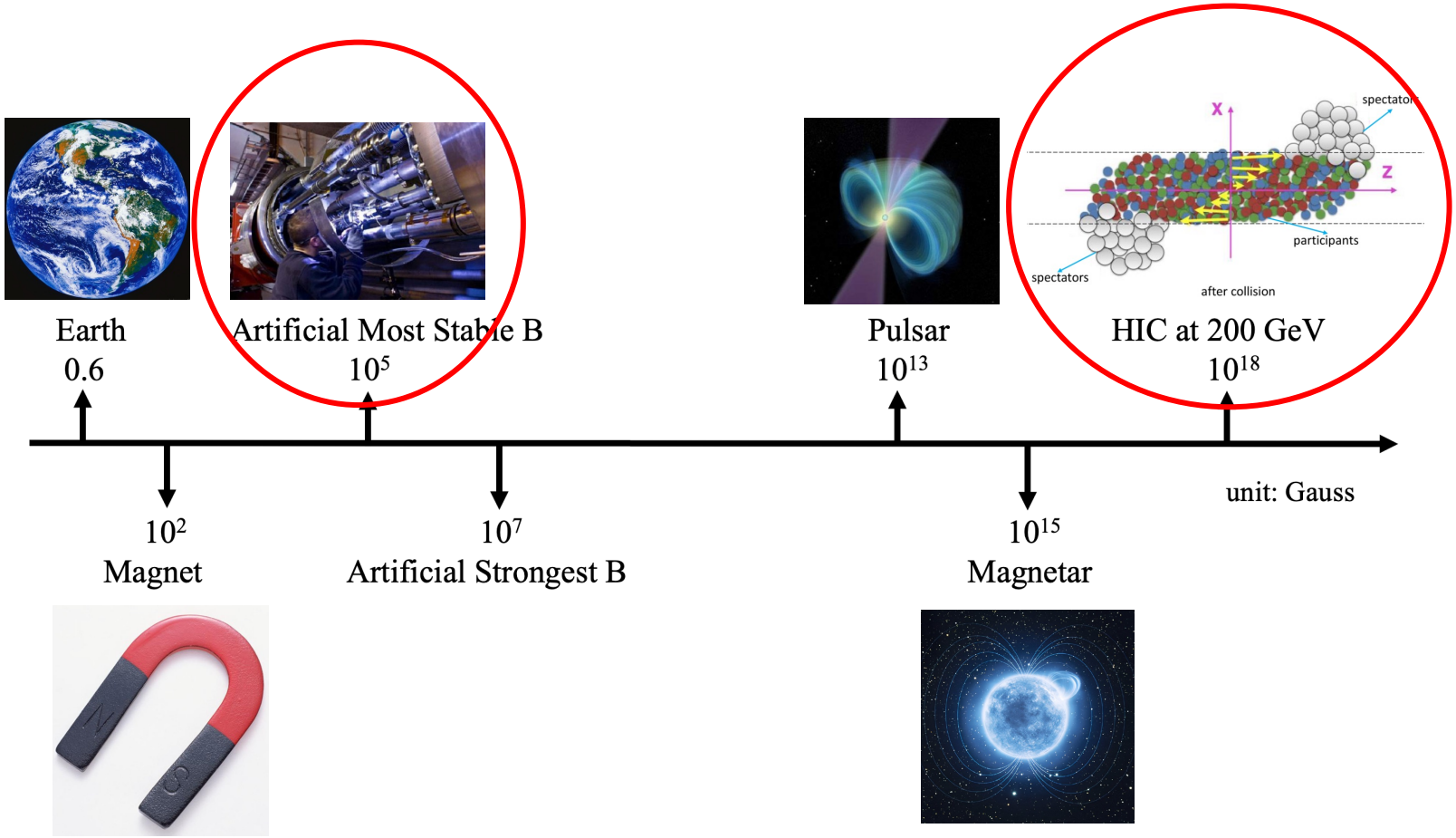

Chiral Magnetic Effect (CME)

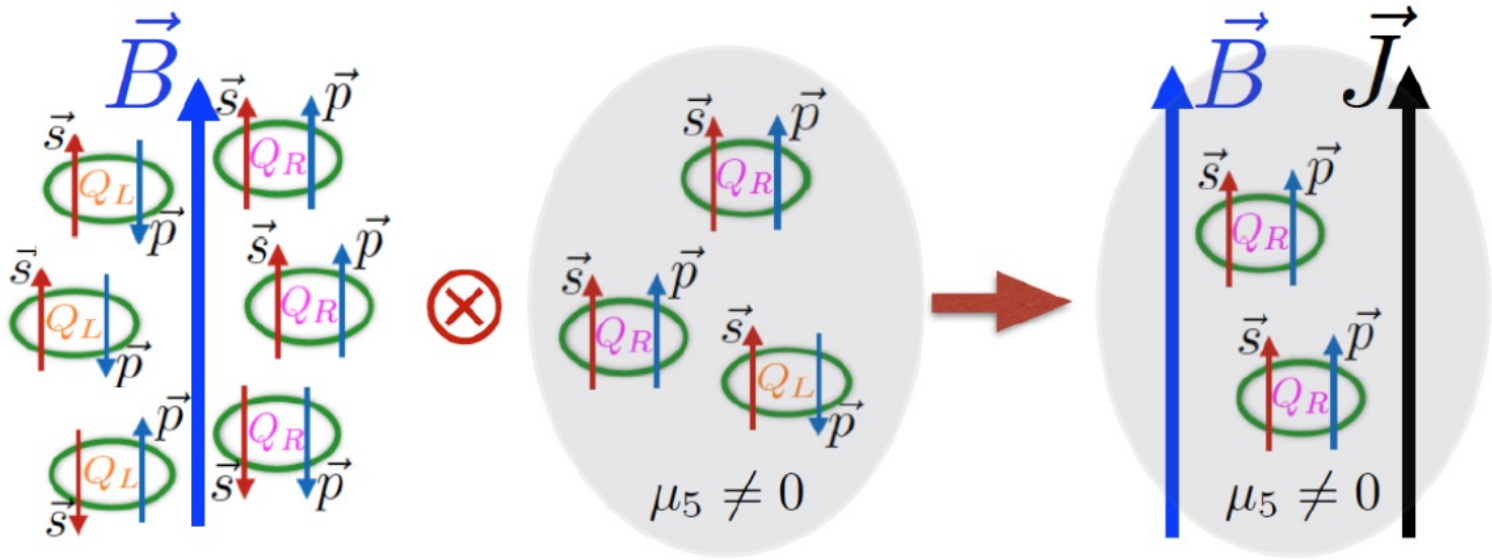

Prog. Part. Nucl. Phys. 88 (2016) 1-28.

$$\vec{J} = \sigma_5 \vec{B} = \left(\frac{(Qe)^2}{2\pi^2}\mu_5\right)\vec{B}$$

Observables: $\gamma \equiv \langle \cos(\phi_\alpha + \phi_\beta - 2\Psi_{\mathrm{RP}}) \rangle$

$$= \langle \cos\Delta\phi_\alpha \cos\Delta\phi_\beta \rangle - \langle \sin\Delta\phi_\alpha \sin\Delta\phi_\beta \rangle \Longrightarrow \Delta\gamma \equiv \gamma^{OS} - \gamma^{SS}$$

$$= (\langle v_{1,\alpha} v_{1,\beta} \rangle + B_{\mathrm{in}}) - (\langle a_{1,\alpha} a_{1,\beta} \rangle + B_{\mathrm{out}})$$

$$\delta \equiv \langle \cos(\phi_\alpha - \phi_\beta) \rangle \Longrightarrow \Delta\delta = \delta^{OS} - \delta^{SS}$$

Isobaric Collisions

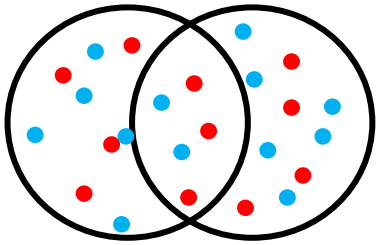

$^{96}_{44}\mathrm{Ru} + {}^{96}_{44}\mathrm{Ru}$

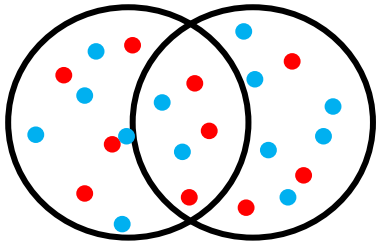

$^{96}_{40}\mathrm{Zr} + {}^{96}_{40}\mathrm{Zr}$

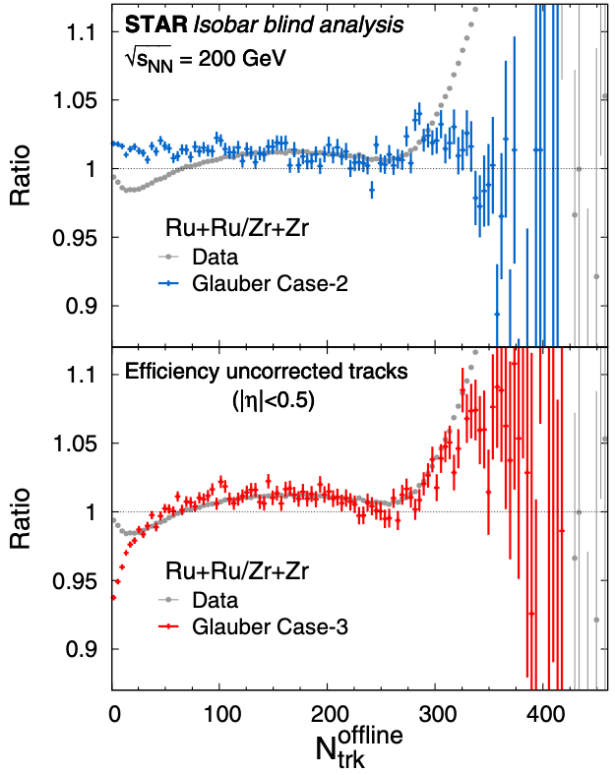

- Ratio≠ 1 ⟹ Different background.
- Different initial nuclear structures, deformation or neutron skin?

Nuclear structure introduced in AMPT

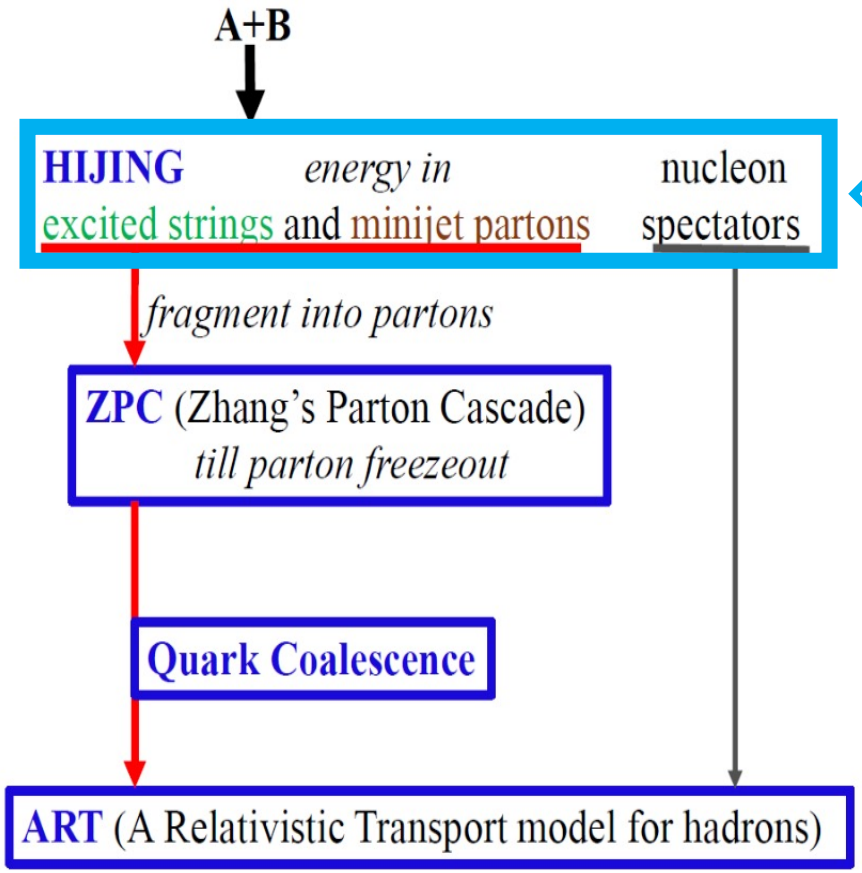

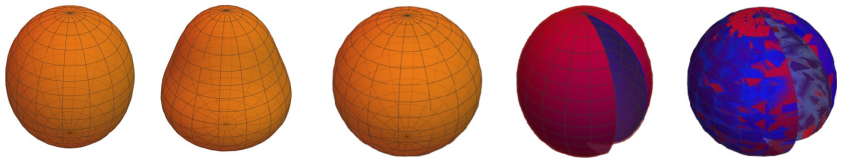

$$\rho(r,\theta,\phi) = \frac{\rho_0}{1+\exp\{\frac{1}{a}(r - R[\theta,\phi])\}}$$

$$R[\theta,\phi] = \boldsymbol{R_0}(1 + \boldsymbol{\beta_2}[\cos\boldsymbol{\gamma}Y_{2,0} + \sin\boldsymbol{\gamma}Y_{2,2}] + \boldsymbol{\beta_3}\sum_{m=-3}^{3}\alpha_{3,m}Y_{3,m} + \beta_4\sum_{m=-4}^{4}\alpha_{4,m}Y_{4,m})$$

Z.W. Lin, et al, Phys. Rev. C 72 (2005) 064901

Results for 18 Cases VS STAR

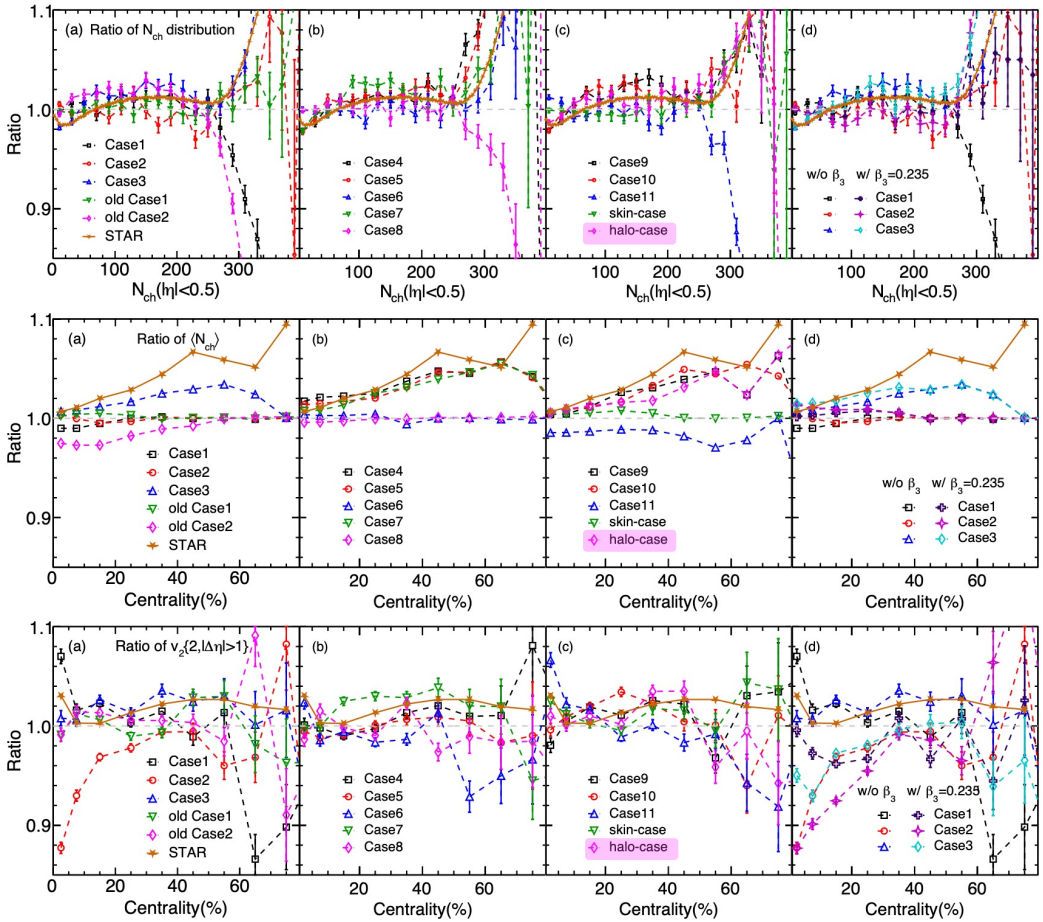

	old Case 1	old Case 2	Case 1	Case 2	Case 3	Case 4
$\langle\chi^2\rangle$	0.204	0.682	0.255	0.400	0.097	0.053
	Case 5	Case 6	Case 7	Case 8	Case 9	Case 10
$\langle\chi^2\rangle$	0.049	0.224	0.051	0.227	0.057	0.048
	Case 11	skin-type	halo − type	Case 1 w/ β_3	Case 2 w/ β_3	Case 3 w/ β_3
$\langle\chi^2\rangle$	0.430	0.177	0.047	0.247	0.506	0.166

Charge Separation in AMPT

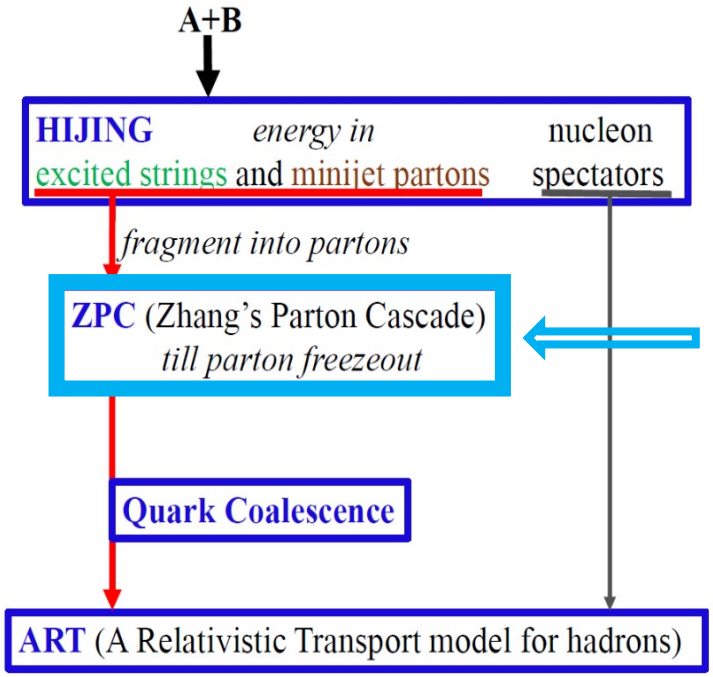

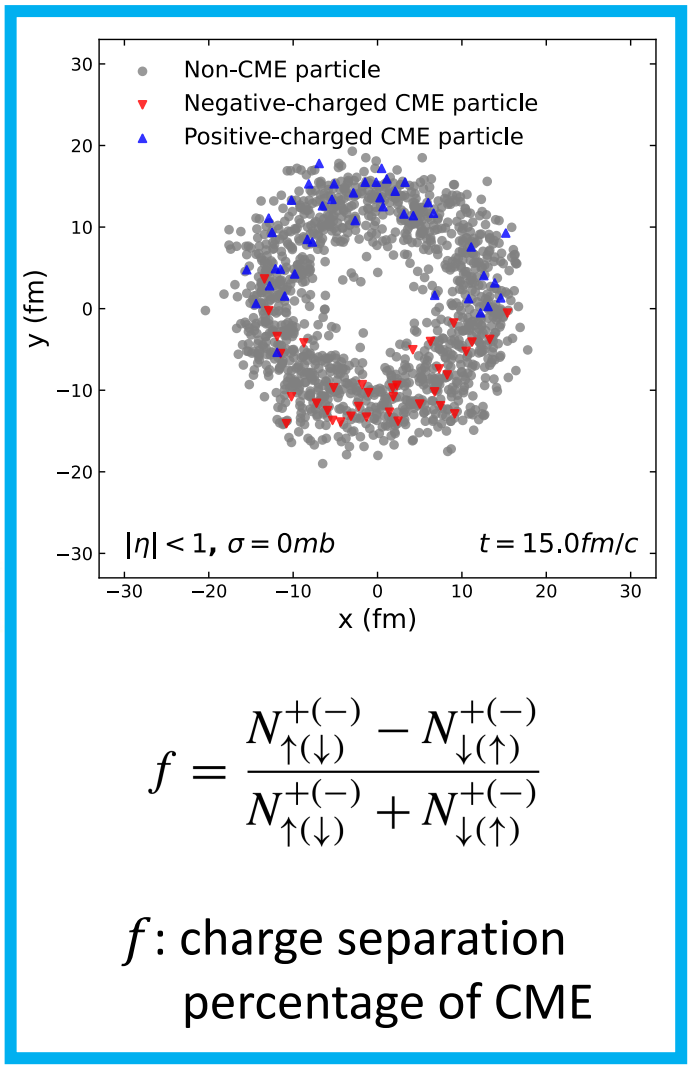

$\approx$

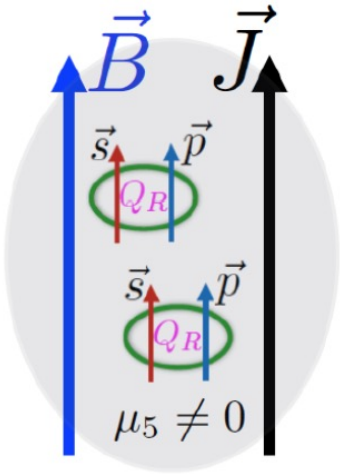

$$f = \frac{N^{+(-)}_{\uparrow(\downarrow)} - N^{+(-)}_{\downarrow(\uparrow)}}{N^{+(-)}_{\uparrow(\downarrow)} + N^{+(-)}_{\downarrow(\uparrow)}}$$

f: charge separation percentage of CME

$$\vec{J} = \sigma_5 \vec{B} = \left(\frac{(Qe)^2}{2\pi^2}\mu_5\right)\vec{B}$$

$f = 0, 2\%, 5\%, 7.5\%, 10\%$ in AMPT.

Halo-Type Results VS STAR

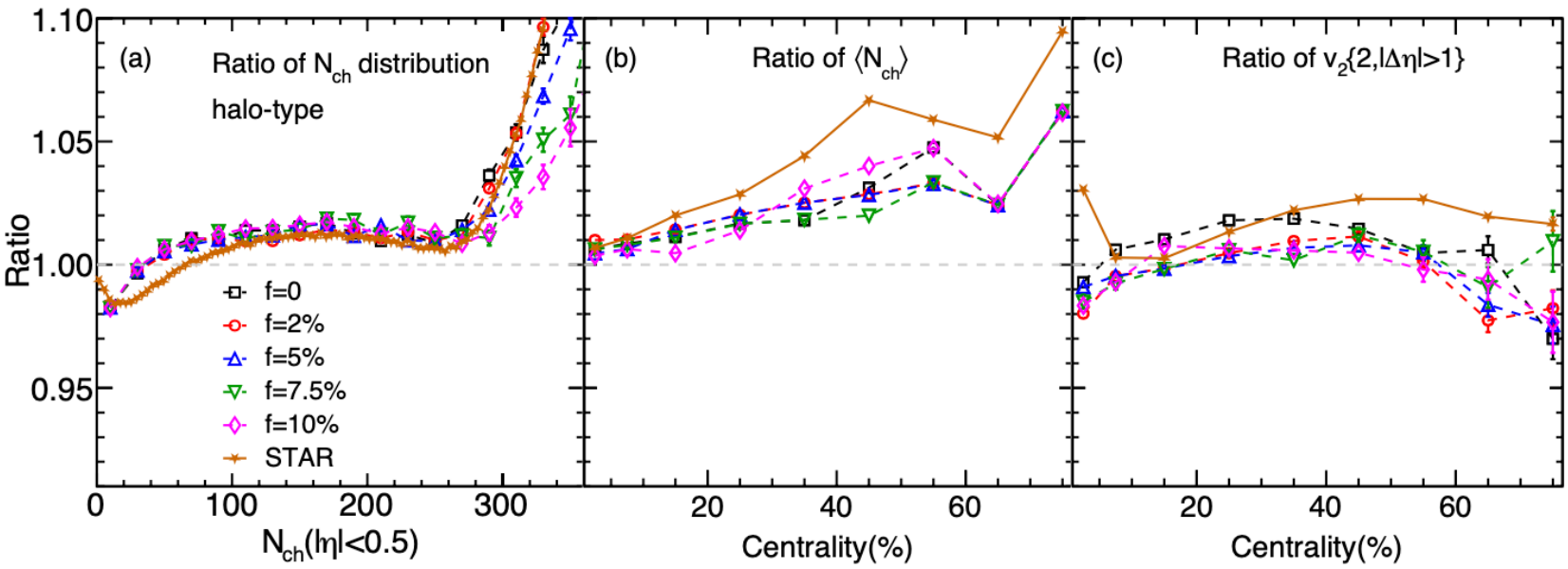

- At central and mid-central collisions, the N_{ch} & v_2 ratios are close to data.
- The ratios have no obvious dependences with respect to f.
- Overall, the results at small f are closer to data.

$\Delta\delta$ with Different f

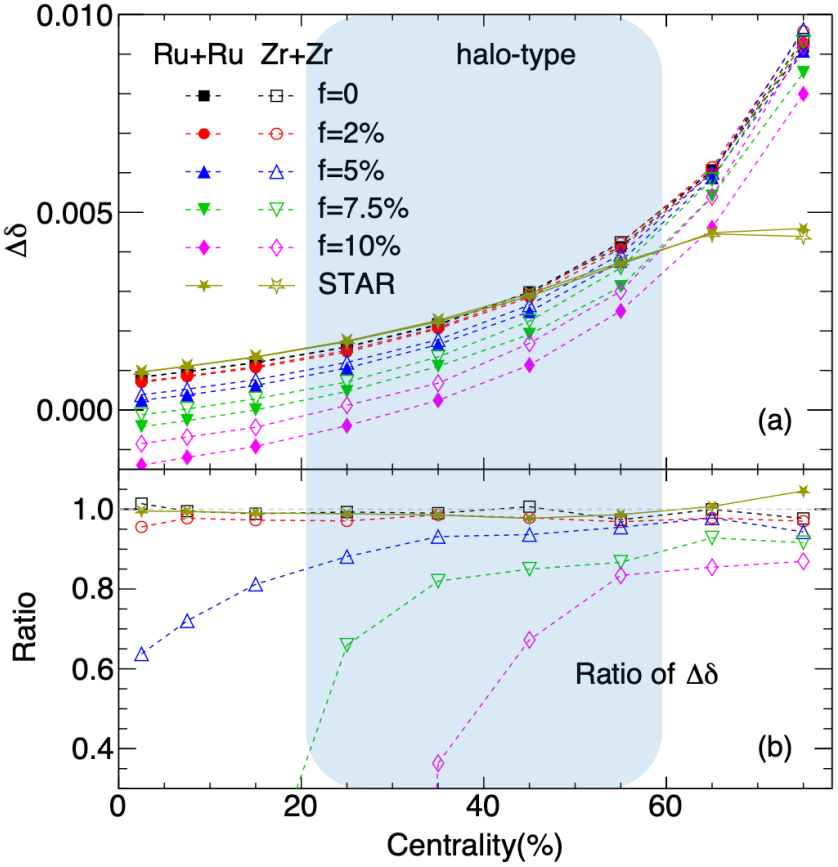

- $\delta \equiv \langle \cos(\phi_\alpha - \phi_\beta) \rangle$, $\Delta\delta = \delta^{OS} - \delta^{SS}$
- At mid-central collisions, $\Delta\delta \propto f$.

$\Delta\delta$ with Different f

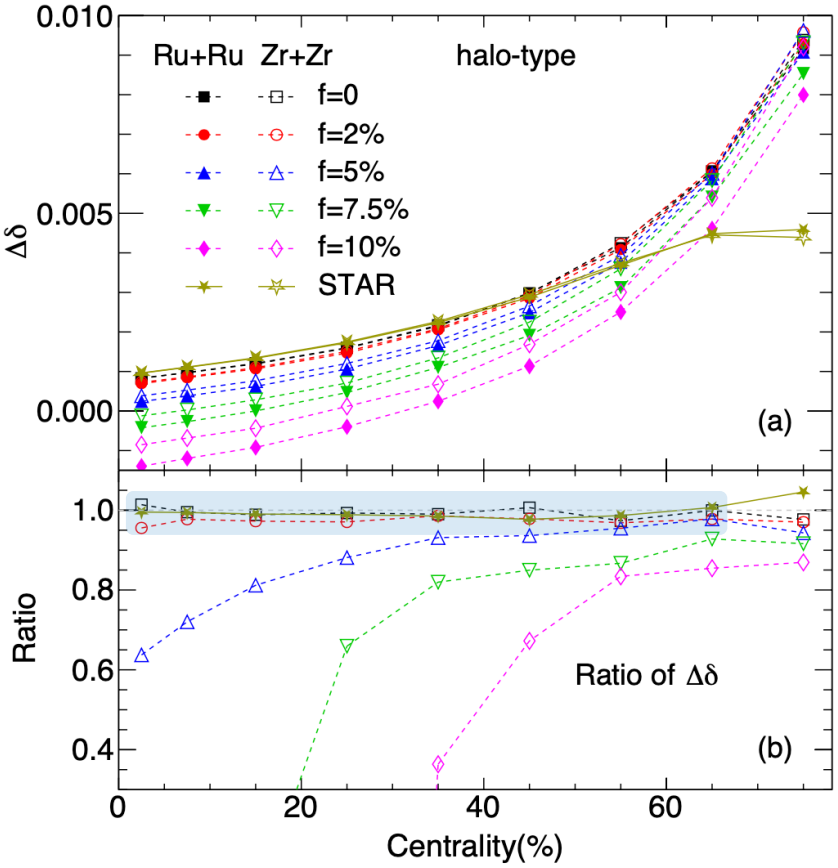

- $\delta \equiv \langle \cos(\phi_\alpha - \phi_\beta) \rangle$, $\Delta\delta = \delta^{OS} - \delta^{SS}$
- At mid-central collisions, $\Delta\delta \propto f$.
- At central & mid-central collisions, $\Delta\delta$ & its ratios are closer to data for $f < 5\%$.

$\Delta\delta$ with Different f

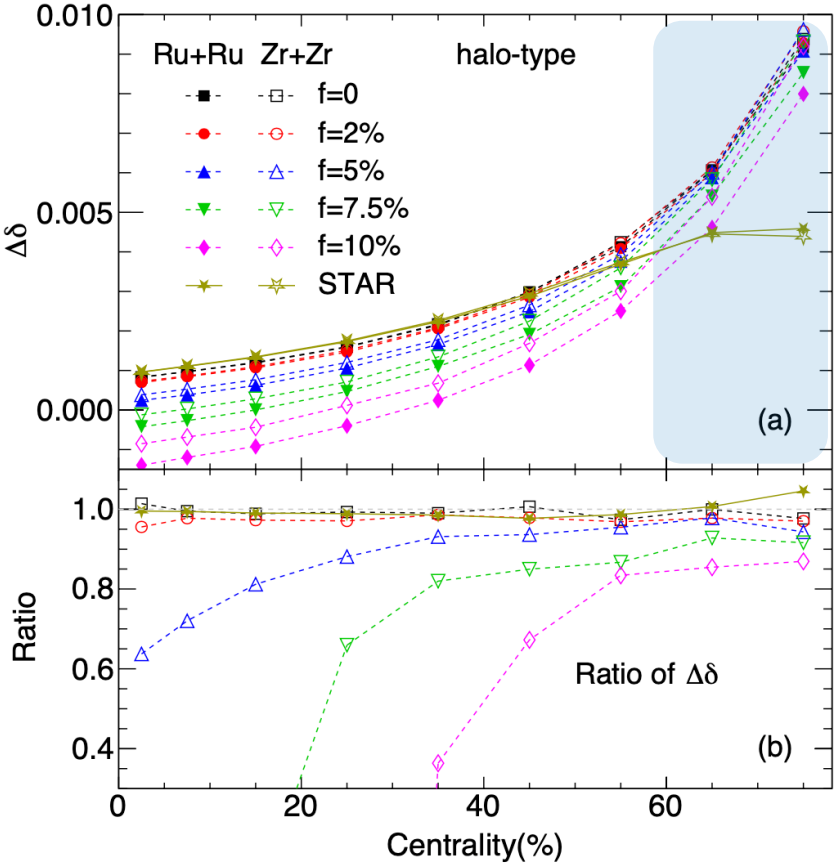

- $\delta \equiv \langle \cos(\phi_\alpha - \phi_\beta) \rangle$, $\Delta\delta = \delta^{OS} - \delta^{SS}$
- At mid-central collisions, $\Delta\delta \propto f$.
- At central & mid-central collisions, $\Delta\delta$ & its ratios are closer to data for $f < 5\%$.
- At peripheral collisions, model results are above the data.

$\Delta\gamma$ w/ Different f

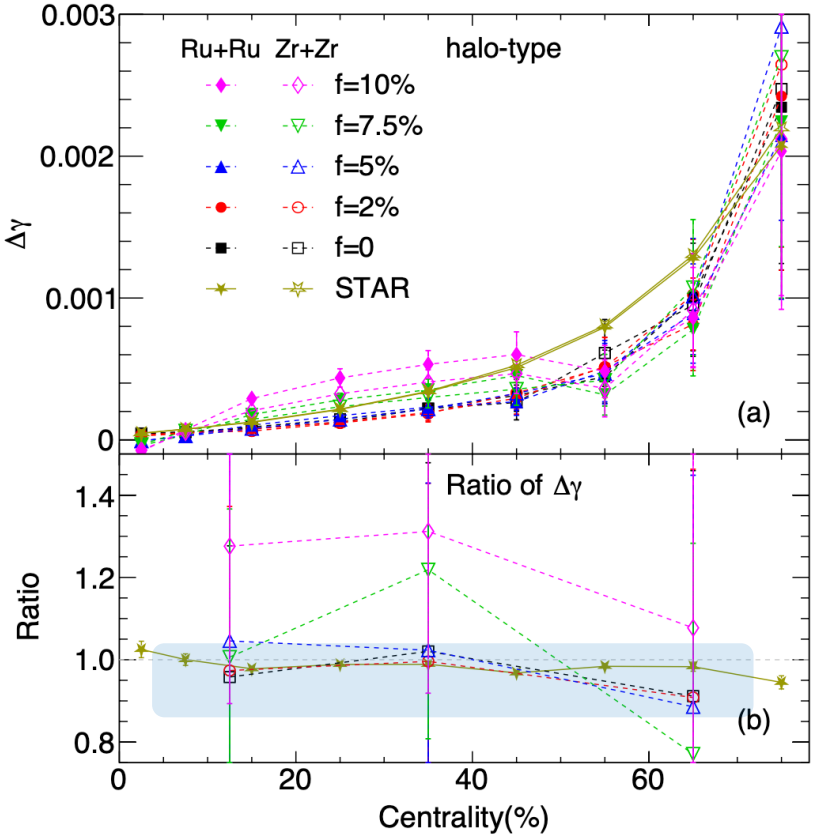

- $\gamma = \langle \cos(\phi_\alpha + \phi_\beta - 2\Psi_{\mathrm{RP}}) \rangle$,

  $\Delta\gamma = \gamma^{OS} - \gamma^{SS}$
- At central & mid-central collisions, $\Delta\gamma$ & its ratios are much closer to data for $f \leq 5\%$.

$\Delta\gamma$ w/ Different f

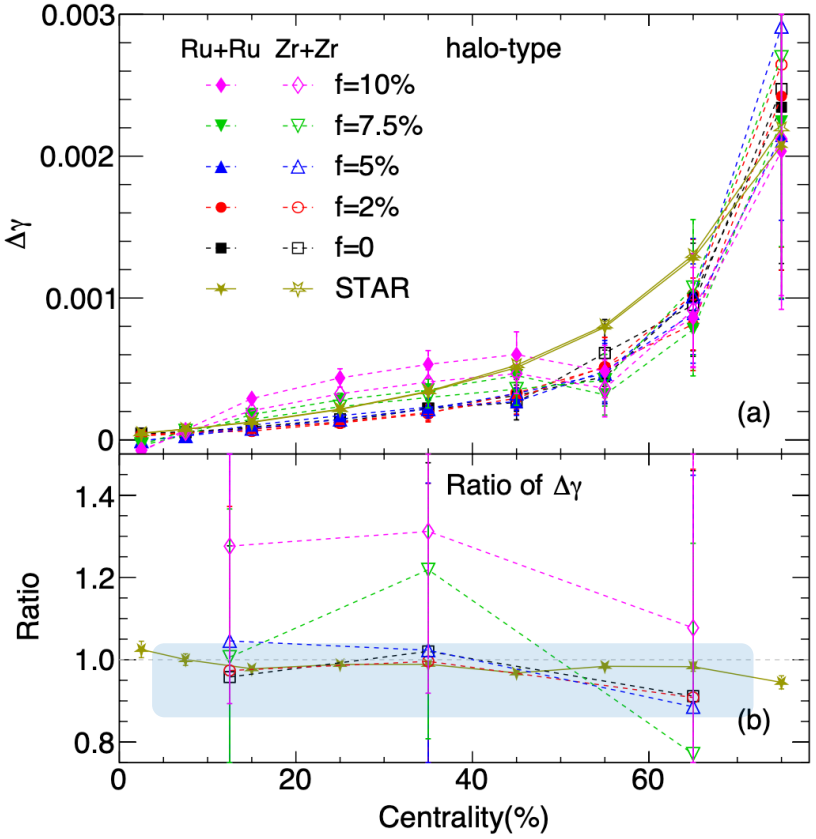

- $\gamma = \langle \cos(\phi_\alpha + \phi_\beta - 2\Psi_{\mathrm{RP}}) \rangle$,

  $\Delta\gamma = \gamma^{OS} - \gamma^{SS}$
- At central & mid-central collisions, $\Delta\gamma$ & its ratios are much closer to data for $f \leq 5\%$.
- The results at $f = 2\%$ & $f = 5\%$ are similar to $f = 0$.
- In isobaric collisions, the CME signal is weak and need to more sensitive observables.

Final State Interaction

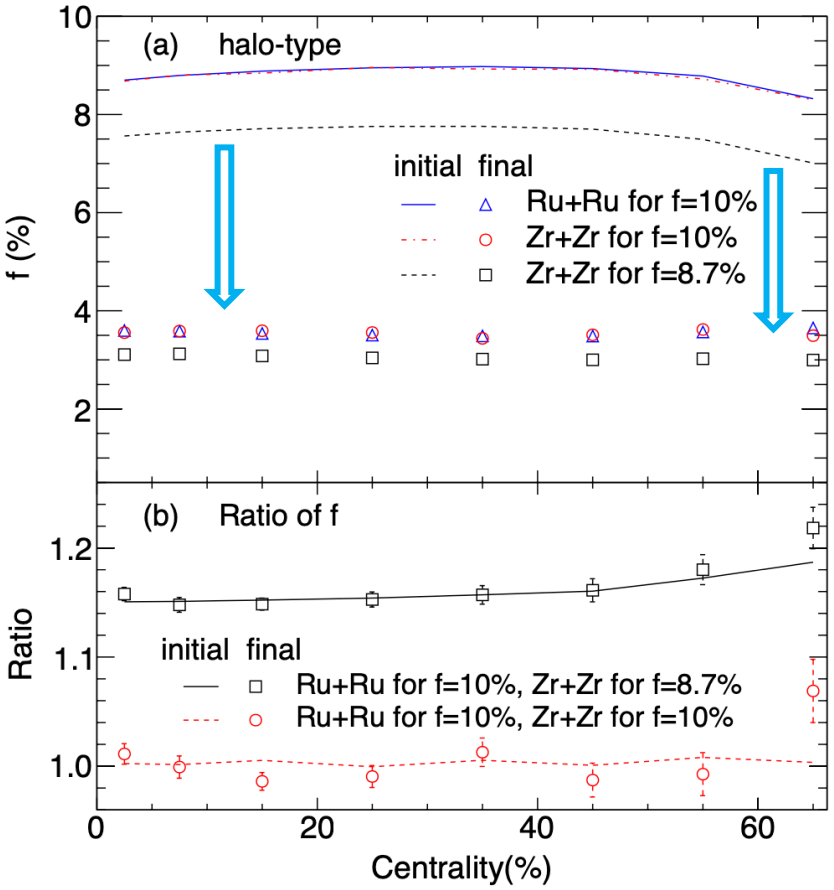

- Final state interactions weaken the CME signal.

Final State Interaction

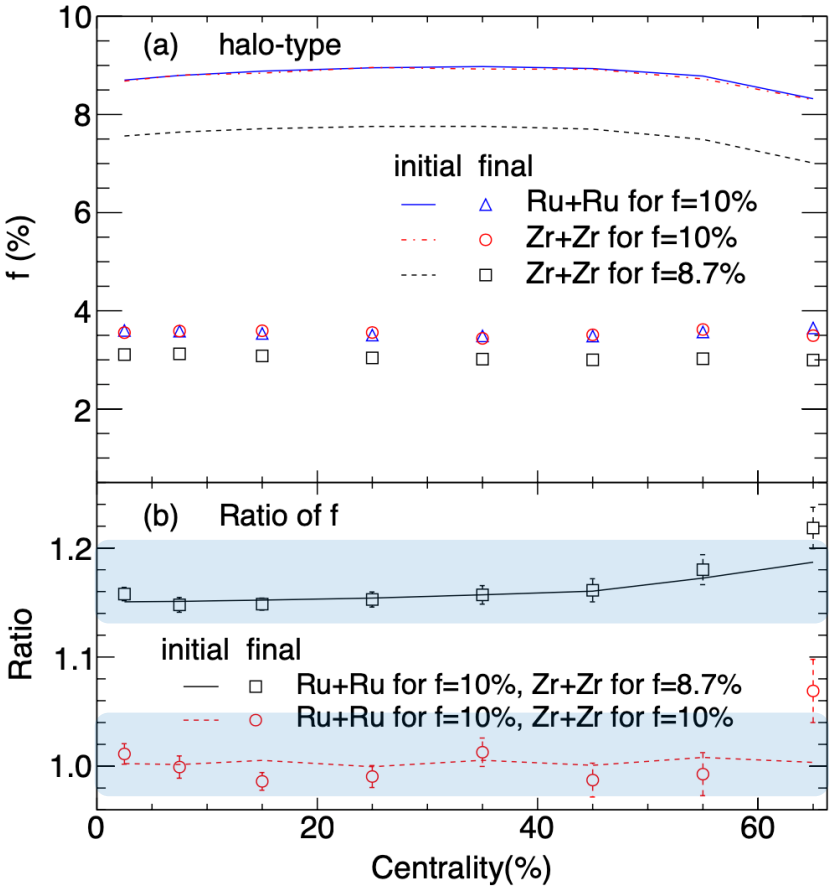

- Final state interactions weaken the CME signal.
- The ratios at initial state are consistent with final state.
- The differences of CME can keep to the final state in isobaric collisions.

Summary

- The neutron-skin has big effect in isobaric collisions.
- $\Delta\delta$ & $\Delta\gamma$ results can be reproduced by AMPT w/o or w/ small CME strength.
- In isobaric collisions, initial CME signal is absent or small.
- Final state interactions significantly weaken the initial CME.
- More sensitive observables are required for searching the possible small CME signal in isobaric collisions.

Summary

- The neutron-skin has big effect in isobaric collisions.
- $\Delta\delta$ & $\Delta\gamma$ results can be reproduced by AMPT w/o or w/ small CME strength.
- In isobaric collisions, initial CME signal is absent or small.
- Final state interactions significantly weaken the initial CME.
- More sensitive observables are required for searching the possible small CME signal in isobaric collisions.

Thank you for your attention!